Wavelet-based high-capacity watermarking of 3-D irregular meshes

William Puech, Meha Hachani, Azza Ouled-Zaïd

▶ **To cite this version:**

William Puech, Meha Hachani, Azza Ouled-Zaïd. Wavelet-based high-capacity watermarking of 3-D irregular meshes. Multimedia Tools and Applications, 2015, 74 (15), pp.5897-5915. 10.1007/s11042-014-1896-3 . lirmm-01233554

HAL Id: lirmm-01233554

https://hal-lirmm.ccsd.cnrs.fr/lirmm-01233554

Submitted on 2 Dec 2015

HAL is a multi-disciplinary open access archive for the deposit and dissemination of scientific research documents, whether they are published or not. The documents may come from teaching and research institutions in France or abroad, or from public or private research centers.

L'archive ouverte pluridisciplinaire **HAL**, est destinée au dépôt et à la diffusion de documents scientifiques de niveau recherche, publiés ou non, émanant des établissements d'enseignement et de recherche français ou étrangers, des laboratoires publics ou privés.

Multimed Tools Appl
DOI 10.1007/s11042-014-1896-3

Wavelet-based high-capacity watermarking of 3-D irregular meshes

A. Ouled Zaid · M. Hachani · W. Puech

© Springer Science+Business Media New York 2014

Abstract Digital watermarking can be used as data hiding technique to interleave cover content with auxiliary information before transmitting and storing applications. While image and video watermarking has been widely studied, much less attention has been paid to its application in 3D mesh models. This is principally due to their intrinsic irregular sampling nature. This paper proposes a high-capacity watermarking scheme for the purpose of inserting meta-data into 3D triangle meshes. Our proposal can be applied to meshes with arbitrary topology by using irregular wavelet-based analysis. The watermark is embedded in an appropriate resolution level by quantizing the norms of wavelet coefficient vectors. To ensure robustness to similarity transformation, a robust synchronization (indexing) mechanism is performed on the 3D model after irregular wavelet analysis. Experimental results show that our watermarking framework is robust to common geometric attacks and can provide relatively high data embedding rate whereas keep a relative lower distortion.

Keywords Three-dimensional meshes · Watermarking · Wavelet transform · Quantization index modulation

1 Introduction

In the last decade, with the interest and requirement of 3-D models in industrial, medical and entertainment applications, 3-D mesh watermarking has received much attention in

A. O. Zaid (✉) · M. Hachani
SysCom Laboratory, University of Tunis El Manar, National Engineering School of Tunis,
B.P. 37, le Belvedere, 1002 Tunis, Tunisia
e-mail: azza.ouledzaid@isi.rnu.tn,azza.ouled-zaid@laposte.net

M. Hachani
e-mail: meha.hachani@gmail.com

W. Puech
LIRMM Laboratory UMR CNRS 5506, 34095 Montpellier Cedex 5 France
e-mail: william.puech@lirmm.fr

Published online: 01 June 2014

the community [2, 7, 27, 28]. Specifically, high-capacity (H-C) mesh watermarking and data hiding systems are sometimes very useful. They carry a large amount of auxiliary information (metadata) in the cover mesh to enhance its utility or to provide an additional service. The challenge is to design H-C watermarking techniques reaching the trade off among imperceptibility (the enrichment process should not alter the perceptual quality of the host mesh), robustness (the metadata resistance against possible attacks) and data payload (the amount of metadata to be inserted).

The existing mesh watermarking algorithms can be subdivided into two classes depending on whether the hidden message is inserted in the spatial domain, by modifying the geometry or the connectivity, or in the transform domain, by modifying the coefficients obtained after a certain transformation.

It is well known that image watermarking methods, based on spectral analysis, provide better robustness and imperceptibility. However, for 3D meshes, there does not yet exist an efficient spectral analysis tool [27]. Besides the direct mesh spectral domain, obtained by direct frequency analysis, we also find embedding algorithms based on multiresolution analysis. In the case of 3-D meshes, multiresolution analysis seems more flexible than the other spectral-like transforms, in sense that it provides different embedding locations that can satisfy different application requirements.

Moreover, the mesh multiresolution analysis based on discret wavelet transform (DWT) is a very suitable tool for constructing an imperceptible and high-capacity watermarking system. Based on the regular wavelet analysis, Kanai et al. [13], proposed a non-blind watermarking algorithm for 3-D meshes. Uccheddu et al. [21] extends [13] to achieve a blind watermark detection. Recently, Wang et al. [26] developed a hierarchical watermarking framework based on wavelet transform of semi-regular meshes. The aforementioned wavelet based watermarking schemes cannot process irregular meshes directly. They can embed the watermark into an irregular mesh by using remeshing that converts an irregular mesh into a semi-regular one. But, the remeshed model cannot be seen as identical to the original, as it corresponds to a different sampling of the underlying 3-D surface. Consequently, the watermark robustness and imperceptibility may be degraded due to this remeshing preprocessing. Using the direct irregular mesh wavelet analysis tool [22], Kim et al. [14] proposed a similar correlation-based scheme as in [21] to embed watermark components in bins (groups) of wavelet coefficient vectors (WCVs). Despite its robustness against various geometric attacks, Kim et al. method is penalized by its limited capacity (the maximal data payload) and quality degradation.

Recently In the present work, we propose a watermarking technique for enrichment applications of 3-D surface meshes. The motivation is to design a blind watermarking system, taking into account the capacity-imperceptibility-robustness requirements. For this purpose, we employ a substitutive embedding approach based on Quantization Index Modulation (QIM) [6] and applied in the wavelet transform domain. Our proposal can be applied to irregular as well as regular meshes by using irregular wavelet analysis introduced by Valette and Prost [22]. The chosen watermarking primitive is the **L2** norm of the geometric wavelet coefficient vector (WCV), at a certain appropriate resolution level. Each **L2** norm is independently quantized to encode one bit of the watermark message.

To ensure invariance of the wavelet coefficients after inverse wavelet transform, we synchronize the connectivity by re-ordering the coefficients depending on the length of the related edges. It is worth mentioning that Kim et al. [14] watermarking algorithm, which is based on an additive approach, synchronizes the connectivity by re-ordering the vertex indexes from a reference vertex. Another important difference is that Kim et al. [14]

algorithm divides the histogram of the **L2** norm of WCVs in the approximation mesh, into regular bins. Each bin is used as unit to insert one bit of the watermark.

The rest of this paper is organized as follows. In Section 2, we provide a brief review of high-capacity mesh watermarking techniques. In Section 3, we explain our watermarking approach in detail. In Section 4, we present the extended version of our embedding scheme to ensure high robustness to some similarity transformations. Next, in Section 5, the particular scenarios simulated are described and the results obtained are presented and discussed. Finally, in Section 6, we conclude and mention potential improvement in future work.

2 Brief review of high-capacity mesh watermarking techniques

The basic idea of high-capacity mesh watermarking is to embed a large amount of additional information within the host model to enrich its content. As a result, high-capacity mesh watermarking schemes can be used in data hiding applications. In particular, blind high-capacity watermarking algorithms are of special interest as they provide automatic retrieving of the payload without any kind of assistance. High-capacity watermarks are often fragile, embedded in the spatial domain, taking the individual vertex coordinates as the watermarking primitives. In their work, Cayre and Macq [5] developed a high-capacity blind data-hiding algorithm for triangular meshes. The chosen watermarking primitive is the projection of a vertex on its opposite edge in a triangle. The embedding capacity is about 0.4 to 0.8 bit/vertex.

Similarly, Maret and Ebrahimi [19] developed a high-capacity method to embed information into the geometry of a 3-D polygonal mesh. To guarantee robustness against rotation, scaling and translation attacks, the model geometry is transformed into a similarity-invariant space resulting in a non-uniformly sampled function on the unit sphere. The resulting samples are then modified in order to embed the message. Simulation results showed that the embedding capacity of the proposed technique is about 0.5 bit/vertex for an error-free extraction. Bors [24] also developed a blind algorithm using the relative position of a vertex to its 1-ring neighbors as primitive. A two-state space division is established and the vertex is assumed to be moved into the correct subspace according to the next watermark bit. Recently, Yang and Yao [28], proposed a high capacity data hiding algorithm that combines the local coordinate system, constructed by the vertex and its 1-ring neighbors with a special quantization technique. Message is embedded by modifying coordinate of the central vertex without changing the coordinate systems.

Wang and Cheng [23] proposed a high-capacity steganographic approach for 3-D polygonal meshes which is characterized by its robustness to affine transformations. An embedding capacity of about 3 bits per vertex, is achieved by applying a multi-level embedding procedure. This procedure consists of modifying successively the parallel, vertical, and rotary positions of a vertex related to its opposite edge in a triangular face. To enhance the invisibility of their embedding method, Cheng and Wang [8] extended their high-capacity mesh watermarking algorithm. The basic idea is to use a new representation rearrangement procedure (RRP) that allows to adaptively embed more bits in rough regions of the mesh surface. Bogomjakov et al. [4] proposed to embed watermarks by modifying the orders of the vertices and faces in the cover mesh. The embedding capacity attains $((\log_2 n!) - n + 1)$ bits on a polygonal mesh of n vertices or faces. Chung et al. [11] realized a high-capacity embedding scheme that consists on rearranging the vertex and face representation information in the cover mesh. For a model with n vertices, the proposed method can yield an embedding capacity of approximately $3 \lg n$ bits per vertex.

Recently, Gao et al. [12] proposed a robust and high capacity watermarking method for 3D Meshes with any topological connectivity. Before the embedding stage, the authors used a cryptographic hash table with a secret key to generate a binary sequence, and then they converted it to an octal sequence. The hidden message is divided into sequential groups. The watermark embedding process is performed in the spatial domain based on affine transformations. Each group of the octal sequence is inserted by slightly modifying the length ratios of one diagonal segment to the residing diagonal intersected by the other one in a coplanar convex quadrilateral. During this stage the quadrilaterals coplanar are keeping unchanged. In the recovery stage, the message is extracted by combining all the sequential groups through majority voting. The proposed approach is considered as affine-transformation-invariant while provides a higher embedding capacity. More Recently, authors in [17] developed a new high capacity hiding algorithm for 3-D polygonal meshes. The hidden message is embedded in the representation domain by modifying both geometry and connectivity information. This approach called representation permutation can embed a large amount of payload (at least 45 bits/per vertex) by permuting vertex/triangle representation orders and connectivity information. The proposed algorithm provides high hiding capacity with negligible distortion.

To summarize, the existing high-capacity mesh watermarking schemes can be classified as geometry-based or order-based methods. The latter naturally leads to a relatively poor robustness, whereas capacity increases. Geometry-based methods can easily achieve the robustness against the content-preserving operations but their capacity is somewhat limited. Wang et al. [26] proposed a blind and high-capacity watermarking scheme that combines the ideas of both kinds of methods. The watermark embedding was specifically proposed for semi-regular meshes and applied on the wavelet transform domain to take advantage of the multiresolution representation. As mentioned above, watermarking methods, based on the multiresolution analysis, are of specific interest since they are able to embed the watermark information in the coefficients of a suitable scale (or resolution), depending on the application requirements.

3 Presentation of the proposed high capacity watermarking framework

In this work, we propose a high capacity watermarking scheme based on multiresolution analysis of meshes with arbitrary topology. Our method considers direct replacement of specific wavelet transform coefficients of the cover mesh using quantization watermarking approach. Specifically, the message is embedded by slightly modifying the norms of WCVs

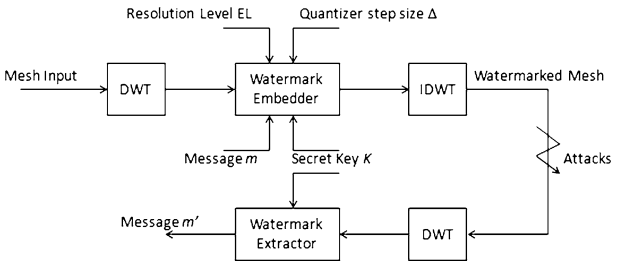

Fig. 1 Main building blocks of the proposed embedding-recovery scheme

associated with a specific resolution level, using non-linear scaling QIM (NLS-QIM) watermark design. The developed watermarking system is depicted in a block diagram form as shown in Fig. 1.

It is worth mentioning that QIM method is a practical implementation of the ideal Costa coding scheme [9]. It is a widely used quantization-based embedding technique for image, audio and video watermarking, due to its ease of implementation, computational flexibility and large data payloads.

3.1 Multiresolution analysis

Multiresolution analysis of 3D meshes is of crucial importance since it gives efficient representation of 3D model at multiple levels-of-detail with many inherent advantages including progressive compression depending on the storage conditions and displaying capacity of the available resource, and level-of-details display accelerating the rendering.

3D mesh multiresolution analysis produces a coarse mesh that represents the basic shape of the model and a list of details information at different resolution levels. During the dual synthesis stage, a series of reconstructed meshes is constructed. The reconstructed meshes represent the same 3-D model but with different resolutions. Wavelet transform is one of the most commonly used multiresolution representation methods. The mathematical formulation of the wavelet analysis and synthesis of 3-D meshes was introduced by Lounsbery et al. [18]. Valette and Prost [22] proposed an irregular subdivision scheme derived from the Lounsbery's approach, allowing multiresolution decomposition of irregularly subdivided triangular meshes. Based on Valette and Prost approach, each face of a mesh can be subdivided into four (Lounsbery approach), three or two faces, or remains unchanged. For a given mesh M^j having n_j faces and v_j vertices, there are 11^{n_j} possible subdivision schemes. In order to apply multiresolution analysis by the wavelet decomposition to the mesh M^j, the subdivision scheme S^{j+1} leads to the mesh M^{j+1} using the following relationship:

$$S^{j+1}\left(M^{j+1}\right) = M^j, \tag{1}$$

Irregular wavelet analysis scheme simplifies the original mesh by reversing the irregular subdivision principle. Once the simplification is complete, one can build a hierarchical relationship between the original mesh M^j and the simplified one M^{j+1} (its approximate). Consequently, the geometry of M^j can be computed by applying the wavelet decomposition, with two analysis filters A^j and B^j. Let's denote by C^j the $v^j \times 3$ matrix giving the coordinates of each vertex of M^j having v^j vertices. To reconstruct C^j from C^{j+1}, it's necessary to calculate the wavelet coefficients in D^{j+1} by using the following equations:

$$\begin{aligned} C^{j+1} &= A^j C^j \\ D^{j+1} &= B^j C^j \\ C^j &= P^j C^{j+1} + Q^j D^{j+1} \end{aligned} \tag{2}$$

with P^j and Q^j designate the synthesis filters.

The (analysis/synthesis) matrix filters A^j, B^j, P^j and Q^j are calculated based on the lifting scheme to make the mesh approximation M^j as close as possible to the original mesh M^{j+1}. The lifting scheme [20] decomposes the filters in simple matrices. Thereby, the analysis stage is deduced from the synthesis one by using simple sign inversion and ordering of these matrices.

In our work, we used the 3-D multiresolution representation proposed in [22] wich is based on irregular subdivisions. By using irregular wavelet analysis, our watermarking scheme can be applied for both regular and irregular 3-D meshes. The proposed embedding/extraction approaches will be discussed throughout the next sections.

3.2 Watermark embedding stage

As cited earlier, our embedding process is based on QIM watermarking approach. In their work, Chen and Wornell [6] presented the dithered quantization as a special case of quantization index modulation (QIM). Let $q(.)$ be a basic quantizer, and m the watermark message. In dither quantization, a dither vector $d(m)$ is added to the host signal s prior to quantization. The number of possible values of m determines the number of required quantizers. Therefore, m acts as an index which is assigned to a fixed quantizer value. The output of the quantization operation is denoted by:

$$x = q(s + d(m)) - d(m) = q^m(s)$$

For binary dither modulation with uniform scalar quantization ($m \in \{0, 1\}$), the output levels of the quantizers are given by:

$$x = \begin{cases} c_k^0 = k \times \Delta + \frac{\Delta}{4} & \texttt{if } m = 0 \\ c_k^1 = k \times \Delta - \frac{\Delta}{4} & \texttt{if } m = 1 \end{cases} \tag{3}$$

where $k \in \mathbb{N}$ and Δ is a quantizer step size. The above dither modulation approach can be extended to a sequence of quantizers $q(s)$, where each q^m is a mapping from the real line $\mathbb{R}$ to a codebook $\mathcal{C} = \{c_1^m, c_2^m, \ldots, c_L^m\}$, where L is the size of codebook. The output values $\{c_k^m, 1 \leq k \leq L\}$ are referred to as reconstruction points. The robustness requirement suggests that all codebooks should be disjoint, otherwise it is not possible to determine the value of m. Due to the distortion constraint and imperceptibility requirement in data hiding applications, the reconstruction points should be close to the host signal. In our work we designed a watermarking scheme, based on dither modulation strategy, meeting these conflicting requirements. For the embedding purpose, we only consider the set $D^j = [d_0, d_1, \ldots, d_{N-1}]^t$ of WCVs associated with the j^{th} intermediate wavelet decomposition level. The Cartesian coordinates of the coefficients d_i, $i \in \{0, \ldots, N-1\}$ are converted to spherical coordinates $[r_i, \theta_i, \phi_i]^t$ where, $r_i = \|d_i\|$ denotes norm of wavelet coefficient vector d_i. It should be noted that the watermark embedding in the spherical coordinate system, especially in the radial component $r_i = \sqrt{x_i^2 + y_i^2 + z_i^2}$, has the advantage to be invariant to rotation and translation attacks.

Let us consider the watermark message as a binary sequence assigned by $m = \{m_0, \ldots, m_i, \ldots, m_{N-1}\}$, with $m_i \in \{0, 1\}$. The watermark message is inserted by quantizing the WCV norms r_i according to $\widetilde{r_i} = \lfloor \frac{r_i}{\Delta} \rfloor \times \Delta$. The binary decision results on two watermarked components c_0 and c_1 depending on the quantizer value Δ and the scaling parameter α. When $m_i = 0$ is considered, the binary decision results on the watermarked component c_0, given by:

$$\begin{array}{ll} \texttt{if } r_i \in [\widetilde{r_i} + \alpha, \widetilde{r_i} + \frac{\Delta}{2} - \alpha] & \rightarrow c_0 = r_i; \\ \texttt{if } r_i \in [\widetilde{r_i}, \widetilde{r_i} + \alpha] & \rightarrow c_0 = \widetilde{r_i} + \alpha; \\ \texttt{if } r_i > \widetilde{r_i} + \frac{\Delta}{2} - \alpha & \rightarrow c_0 = \widetilde{r_i} + \frac{\Delta}{2} - \alpha; \end{array} \tag{4}$$

Otherwise, if $m_i = 1$ is considered, c_1 is given by:

$$\begin{array}{ll} \texttt{if} \;\; r_i \in [\widetilde{r_i} + \frac{\Delta}{2}, \widetilde{r_i} + \frac{\Delta}{2} + \alpha] & \rightarrow c_1 = \widetilde{r_i} + \frac{\Delta}{2} + \alpha; \\ \texttt{if} \;\; r_i \in [\widetilde{r_i} + \frac{\Delta}{2} + \alpha, \widetilde{r_i} + \Delta - \alpha] & \rightarrow c_1 = r_i \\ \texttt{if} \;\; r_i > \widetilde{r_i} + \Delta - \alpha & \rightarrow c_1 = \widetilde{r_i} + \Delta - \alpha; \end{array} \tag{5}$$

This results in the watermarked component $r_i^{'}$, that yields maximum correlation with r_i for a given scaling parameter α. The use of non linear scaling results in shifted versions of the reconstruction points, which are highly correlated with the original host components. It is worth mentioning that this modification of the embedding algorithm does not affect the watermark robustness ensured by the basic QIM watermarking design.

Based on the work presented in [6], the probability density functions of the quantization error, in the QIM scheme, are assumed to be similar. Consequently, during the recovery step, the distortion-compensation is considered as noise and is statistically independent of the embedded message m. A decrease of scaling parameter α, leads obviously to better robustness under channel perturbations. But, increases the interference, due to the distortion-compensation. To alleviate this problem, authors in [6] use the scaling parameter α that maximizes the "signal-to-noise ratio" which is given by the following formula:

$$SNR = \frac{d_1^2/\alpha^2}{(1-\alpha)^2 \frac{D_s}{\alpha^2} + \sigma_n^2}, \tag{6}$$

being SNR the ratio between the squared minimum distance among quantizers and the overall interference energy that results from distortion-compensation interference and channel interference. d_1 corresponds to the minimum distance for $\alpha = 1$. As a results, the optimal scaling parameter α, that maximizes the SNR, is giving by the following expression:

$$\alpha_{optimal} = \frac{\frac{D_s}{\sigma_n^2}}{\frac{D_s}{\sigma_n^2} + 1}, \tag{7}$$

where $\frac{D_s}{\sigma_n^2}$ denotes the distortion, due to the embedding process. In our embedding scheme, we propose to use the aforementioned concept, introduced by Chen and Wornell [6], regarding the α parameter, in order to minimize the induced distortion while keeping a good trade-off between imperceptibility and watermark message resistance.

3.3 Watermark recovery stage

We have developed a blind watermarking system, so the recovery stage is only made from watermarked mesh without needing the original mesh. A given reconstructed WCV norm $\acute{r_i}$, positioned in the same resolution level chosen for the embedded stage j, is manipulated using (8) to obtain Q^0 and Q^1 indices.

$$\begin{array}{l} Q^0 = \lfloor \frac{\acute{r_i}}{\Delta} \rfloor \\ Q^1 = \lfloor \frac{\acute{r_i} + \frac{\Delta}{2}}{\Delta} \rfloor \end{array}. \tag{8}$$

At this step, we measure the distance between $\acute{r_i}$ and its approximation, as follows:

$$\begin{array}{rl} \texttt{if} \;\; |\acute{r_i} - (Q^1 \times \Delta)| < |\acute{r_i} - (Q^0 \times \Delta)| & \rightarrow m_i = 1 \\ \texttt{else} & \rightarrow m_i = 0 \end{array} \tag{9}$$

The capacity of our watermarking approach is equal to the number of wavelet coefficients N in the considered resolution level. In our experiments, the embedding level (EL) corresponds to the third resolution level ($j = 3$).

4 Preprocessing of wavelet coefficient vectors

Despite its efficiency, our embedding method is vulnerable to similarity transformation, which is considered as content-preserving operation. Indeed, similarity transformation is considered as routine operation since it does not affect the mesh shape. To be invariant to this kind of attack, one just needs to make the watermark synchronization scheme independent of the combinatorial element orders represented in the mesh file.

As an extension to our embedding scheme, we propose to establish a robust synchronization (indexing) mechanism. A re-ordering process is applied on the 3-D model after irregular wavelet analysis. In more detail, the re-ordering is performed on the N wavelet coefficient vectors, localized in the j^{th} resolution level that was selected for embedding purpose. The wavelet coefficients are indexed according to the lengths of their associated edges. First, we sort the edge lengths in ascending order, then we reorder the N WCVs according to the edge length indices. Next the cartesian coordinates of the re-ordered coefficients are converted to spherical coordinates to apply the quantization based embedding as explained in Section 3.2. The inverse re-ordering of the preprocessed WCVs is required in order to apply the inverse DWT and obtain the watermarked 3-D mesh. Figure 2 depicts the extended version of our high capacity watermarking approach, taking into account the re-ordering strategy.

It is worth pointing out that even with the re-ordering of the wavelet coefficients, the proposed embedding method is not invariant to all the content-preserving operations, because the norm of wavelet coefficient (the watermarking primitive) is not invariant to uniform scaling. The re-ordering only makes the algorithm invariant to vertex re-ordering.

5 Experimental results

We have tested our high-capacity watermarking algorithm on several irregular meshes: Venus (100759 vertices), Rabbit (70658 vertices), Horse (112642 vertices), Bunny (34835 vertices). Quality assessment was carried out using two evaluation criteria, maximum root mean square error (MRMS) [3], and mesh structural distortion measure (MSDM) [15]. The

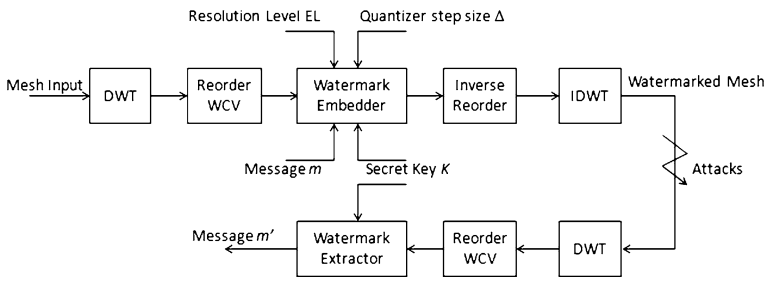

Fig. 2 Extended version of our embedding-recovery scheme

MRMS is an objective surface-to-surface distance between the original mesh M and its modified version M'. It is defined as follows:

$$d_{MRMS} = \max(d_{RMS}(M, M'), d_{RMS}(M', M))$$

where $d_{RMS}(M, M')$ is the root mean square error (RMS) from M to M' given by:

$$d_{RMS}(M, M') = \sqrt{\frac{1}{|M|}\int\int_{p\in M} d(p, M')^2 dM},$$

with p is a point on surface M, $|M|$ is the area of M, and $d(p, M')$ designates the point-to-surface distance between p and M'. It is important to note that the RMS distance is not symmetric.

The MSDM [15] is a perceptual metric that measures the perceptual distance between two 3D models. It is based on the concept of structural similarity that was proposed by Wang et al. [25] for 2D image quality assessment. The robustness is evaluated by the normalized correlation (*corr*) [10] between the extracted binary message and the original embedded one. The correlation coefficient between recovered watermark bits $m_n^{"}$ and the original watermark m_n is calculated by means of

$$corr(m_n^{"}, m_n) = \frac{\sum_{n=0}^{N-1}(m_n^{"} - \bar{m}^{"})(m_n - \bar{m})}{\sqrt{\sum_{n=0}^{N-1}(m_n^{"} - \bar{m}^{"})^2 \times \sum_{n=0}^{N-1}(m_n - \bar{m})^2}} \tag{10}$$

where $\bar{m}$ indicates the average of the watermark and $corr$ varies in the range of $[-1, 1]$.

It is well known that for 3-D mesh watermarking, transform-domain-based techniques that modify the low frequency parts are both more robust, to signal processing attacks, and more imperceptible than the other techniques. On the other hand, towards the medium and high frequencies, the number of wavelet coefficients increases. The purpose of our method is to embed a large amount of information in the cover mesh while maintaining a good compromise between the imperceptibility and the robustness.

Concerning the parameter setting, for the QIM based embedding, we tested several settings of the quantized value Δ and the scaling parameter α. For all tested values, the watermark was entirely recovered without any confusion with a binary error rate (BER) of a NULL value ($corr = 1$). Nevertheless, the use of largest Δ and α values was paid by noticeable mesh quality degradation. In the following tests, the quantizer step size Δ and the scaling parameter α are fixed at 8 and 0.2 respectively. This choice, offers the best compromise between robustness and watermark invisibility.

To understand the impact of the selected EL on imperceptibility and data payload we compared our algorithm's performance with itself at different resolution levels (EL). In our experiments, the watermark message length corresponds to the number of wavelet coefficients in the considered EL. Six resolution levels have been tested for embedding. It should be noted that the total number of resolution levels is dependent on the number of vertices of original mesh. Tables 1 and 2 present payload, MRMS and MSDM variation as function of the considered EL. Based on results reported in these tables, we can notice that the obtained MRMS values increase with the EL. This is principally due to the fact that modification of wavelet coefficients, at high resolution levels, for the embedding purpose will induce modification of the positions of the involved vertices at the lower resolution levels, resulting on high-amplitude objective modifications. It can also be observed from the tables that MSDM perceptual distances between the watermarked and original models decreases for the upper embedding levels. This can be explained by the fact that the amount of induced distortion in

Table 1 Payload, MRMS and MSDM results of embedding binary messages with varying embedding resolution level for Vennus and Rabbit meshes

Model	Vennus			Rabbit		
EL	Payload (kbits)	MRMS (10^{-3})	MSDM	Payload (kbits)	MRMS (10^{-3})	MSDM
1	54.55	0.17	0.14	51.75	0.27	0.077
2	23.47	0.19	0.08	12.93	0.34	0.068
3	**10.65**	**0.2**	**0.04**	**3.23**	**0.38**	**0.021**
4	4.82	0.22	0.03	0.8	0.39	0.02
5	2.21	0.22	0.02	0.2	0.44	0.015
6	1.13	0.24	0.02	0.03	0.41	0.011

low frequency localisations does not degrade too much the visual quality of the deformed object.

Since the watermark message length corresponds to the number of wavelet coefficients in the considered resolution level, the watermark payload decreases rapidly with the increase of EL. In the next subsections, the 3^{rd} resolution level, which leads to a satisfactory compromise between distortion and payload, is considered for embedding purpose.

5.1 Basic simulations

Tables 3 and 4 illustrate the baseline evaluations of the proposed H-C watermarking scheme. From the results reported in these tables, it can be seen that, for all the tested 3D models, our method introduces relatively high-amplitude deformation while keeping it imperceptible (the induced MSDM is less than 0.078). This point is also confirmed in Fig. 3, where three close-ups of original and watermarked meshes are depicted. We can hardly observe any visual difference between the cover and watermarked models. In practice, perceptual distortion measurement is considered more important than the objective distortion measurement since it does not always correctly reflect the visual difference between two meshes. It is worthwhile pointing out that 3D mesh applications have different constrains on the objective and perceptual distortions caused by the watermark insertion. For example, computer-aided

Table 2 Payload, MRMS and MSDM results of embedding binary messages with varying embedding resolution level for Vennus and Rabbit meshes

Model	Vennus			Rabbit		
EL	Payload (kbits)	MRMS (10^{-3})	MSDM	Payload (kbits)	MRMS (10^{-3})	MSDM
1	21.52	0.24	0.074	84.48	0.32	0.063
2	6.82	0.26	0.024	21.12	0.36	0.057
3	**2.91**	**0.3**	**0.024**	**5.28**	**0.4**	**0.038**
4	1.36	0.32	0.023	1.32	0.47	0.034
5	0.63	0.33	0.023	0.33	0.51	0.031
6	0.29	0.34	0.021	0.055	0.56	0.028

Table 3 Baseline evaluations of the proposed watermarking framework and Wang's methods for Venus, Rabbit and Horse meshes (in the parentheses are the results of Wang *et al* H-C watermarking method [26])

	Venus	Rabbit	Horse
EL	3 (4)	3 (4)	3 (4)
Payload (kbits)	10.65 (7.632)	3.23(3.18)	5.28(5.247)
MRMS (10^{-3})	0.2 (0.22)	0.38(0.2)	0.4(0.15)
MSDM	0.04 (0.045)	0.021 (0.039)	0.038(0.058)
corr	1 (1)	1 (1)	1 (1)

design and medical imaging applications require a very small objective distortion, while the visual quality of the watermarked model is generally less important. On the contrary, in digital entertainment applications, the induced distortion should not be noticeable by human eyes, while the amount of the objective distortion is of minor importance.

The results reported in Tables 3 and 4 also compare the data payload, the watermark correlation (*corr*), and the MRMS measures provided by our method with those provided by two existing watermarking methods (without any robustness consideration): Wang et al. method [26] (for Venus, Rabbit, Horse meshes), and Lee et al. method [16] (for Horse, Bunny, and Venus meshes). It should be noted that in the case of Wang et al. watermarking algorithm, the tested mesh is first remeshed to construct a semi-regular mesh before passing through the wavelet decomposition process. The watermarking algorithm presented in [16] consists in modifying the vertices geometry information based on histogram bin shifting.

Figure 4 illustrates the maps of the objective distortions between original and watermarked Rabbit mesh using our method and Wang et al. watermarking scheme [26]. The distance between original and watermarked mesh varies from 0 to 0.001. From Fig. 4, we can see that the distortion introduced by our embedding scheme is globally well balanced. Compared to Wang et al. scheme, the distortion induced by our method is of low frequency.

5.2 Robustness under geometric attacks

In this section, we assess the resistance of the embedded message under various geometric attacks, including noise addition, smoothing, and lossy compression. Surface smoothing is a common operation used to remove the noises introduced during the mesh generation process but in this case significant shape distortion may be introduced. The Laplacian smoothing aims to move the vertices positions based on local information such as the neighbor positions without changing the connectivity of the faces. Only internal vertices

Table 4 Baseline evaluations of the proposed watermarking framework and Lee's methods for Horse, Bunny and Venus meshes (in the parentheses are the results of Lee et al. [16] method)

	Horse	Bunny	Venus
EL	3	3	3
Payload (kbits)	5.28 (0.051)	2.91(0.072)	10.65(0.128)
MRMS (10^{-3})	0.4 (1.03)	0.3(1.52)	0.2(1.77)
MSDM	0.038	0.024	0.04
corr	1 (0.98)	1 (0.98)	1 (0.85)

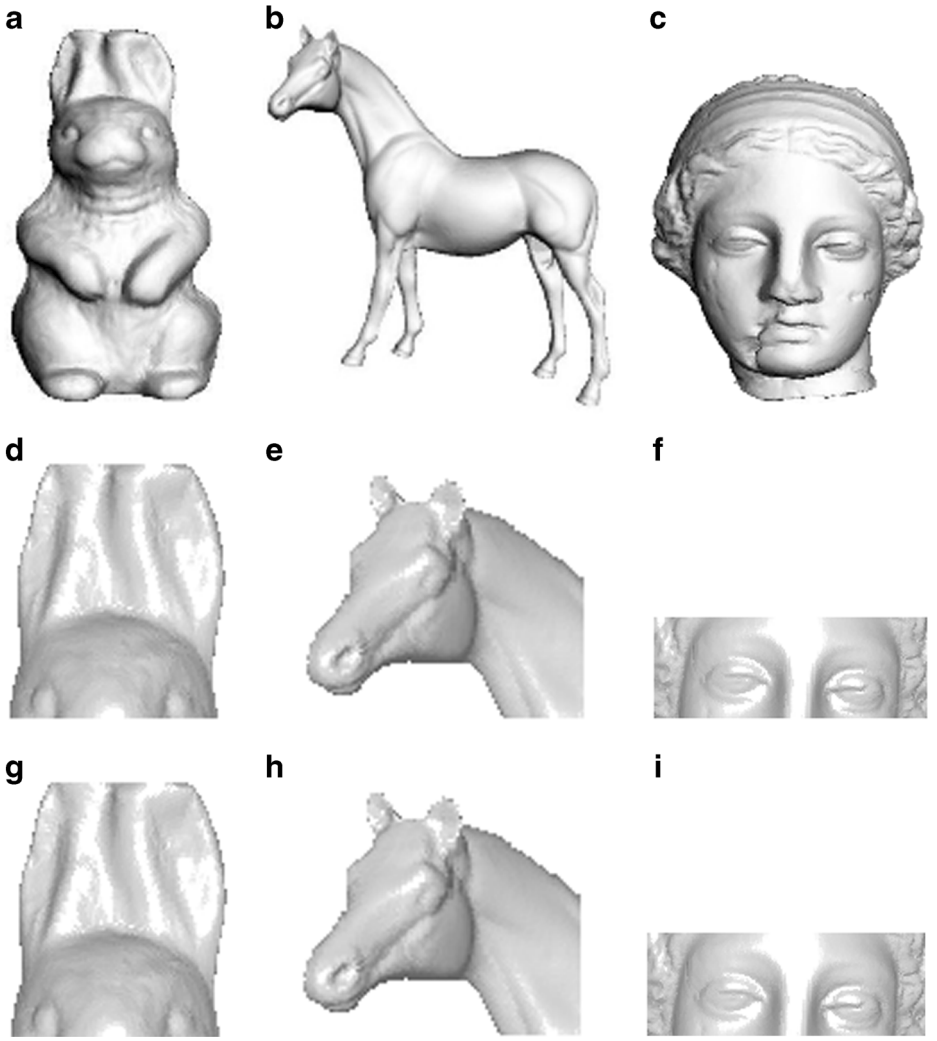

Fig. 3 The original irregular meshes **a** Rabbit, **b** Horse, and **c** Venus. The corresponding close-ups of the original irregular meshes are provided as **d–f**. The corresponding close-ups of the watermarked meshes are also provided as **g–i** for comparison

are simultaneously moved while keeping the boundry vertices positions. Indeed, Laplacian smoothing is an iterative process. In each step, the vertices converge to the barycenter of their neighbors. The shape undergoes significant deformations whenever a large number of Laplacian smoothing iterations are performed. In our work, we retained a Laplacian smoothing with different iteration numbers, and we have chosen to add pseudo-random noises on vertex coordinates. Tables 5, 6 and 7 presents the robustness evaluation results of our method, regardless WCV index re-ordering step , in terms of the normalized correlation ($corr$). The distortion induced by attacks is also measured by MRMS and MSDM measures. The results of the robust watermarking method in [26], based on manifold harmonics transform, are presented in parentheses. It can be seen that with a roughly

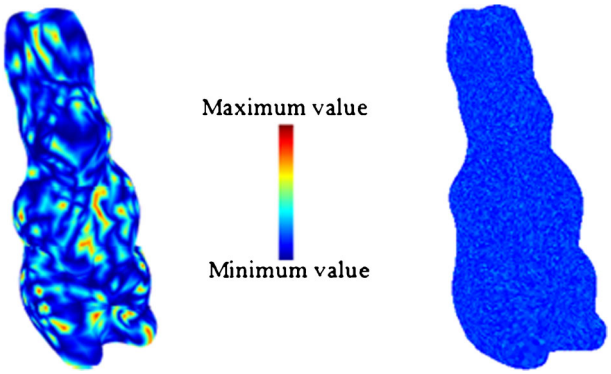

Fig. 4 Maps of the objective distortions introduced by our method (*right side*) and Wang et al. scheme (*left side*)

comparable robustness level, Wang et al. [26] embedding technique introduces higher geometric and perceptual distortions than our method. Additionally, the watermark message length is relatively short, of about 64 bits, which is still negligible compared to our watermarking approach's capacity. Consequently, we can assume that our watermarking scheme has a better trade-off between the robustness, the induced distortion and the capacity payload.

In Table 8, the robustness and imperceptibility of our system, integrating the re-ordering process, are evaluated. Compared with the results reported in Tables 5, 6 and 7, we can notice that the WCVs re-ordering brings on a slight improvement of the watermark imperceptibility. Furthermore, the gain in terms of robustness is notable. When comparing our results with those obtained by the method of Lee et al., we find that our embedding system exhibits superior robustness and quality performance. Also, based on the results reported in Table 4, the reference method is limited to watermarks with very small data payloads of about 52 bits for Horse mesh, which still negligible compared to our watermarking approach's capacity (about 5406 bits for the same mesh).

Table 5 Robustness against the random additive noise addition (in the parentheses are the results of Wang et al. robust watermarking method [26])

Model	Noise	*corr*	MSDM
	0.05 %	0.99 (0.85)	0.097 (0.28)
Venus	0.25	0.99 (0.59)	0.108 (0.7)
	0.5 %	0.99 (0.31)	0.119 (0.83)
	0.05 %	0.99 (0.92)	0.099 (0.18)
Rabbit	0.25 %	0.99 (0.59)	0.105 (0.6)
	0.5 %	0.99 (0.31)	0.111 (0.77)
	0.05 %	0.99 (0.69)	0.105 (0.23)
Horse	0.25 %	0.99 (0.5)	0.114 (0.64)
	0.5 %	0.98 (0.08)	0.12 (0.78)

Table 6 Robustness against the Laplacian smoothing in the parentheses are the results of Wang et al. robust watermarking method [26]

Model	Iterations	*corr*	MSDM
	10	0.99 (0.74)	0.101 (0.15)
Venus	30	0.99 (0.71)	0.117 (0.27)
	50	0.98 (0.62)	0.135 (0.34)
	10	0.99 (0.90)	0.08 (0.15)
Rabbit	30	0.99 (0.71)	0.11 (0.26)
	50	0.99 (0.45)	0.142 (0.31)
	10	0.99 (0.97)	0.092 (0.15)
Horse	30	0.99 (0.5)	0.102 (0.23)
	50	0.99 (0.35)	0.135 (0.28)

5.3 Watermark robustness under similarity transformation

Similarity transformation is considered as a common geometry operation on a 3-D mesh rather than a malicious attack. To achieve invariance of our watermarking method to this routine operation we extended our embedding technique by integrating the re-ordering process which was discussed in detail in Section 4.

To assess the robustness of our method against the similarity transformation, we applied the operations of translation, rotation and uniform scaling on watermarked meshes. Table 9 presents the obtained robustness evaluation results against the considered operations. It can be observed that experimentally our extended scheme possesses a strong robustness to translation and rotation transformations. However, the attack-induced distortions, in terms of MRMS and MSDM, are very high. The results reported in Table 9 also confirm what was said in Section 4 about the low resistance against uniform scaling.

5.4 Robustness under connectivity attacks

Table 10 shows the robustness results of our method, in terms of normalized correlation (*corr*), against connectivity attacks. For comparison purpose, the results of the

Table 7 Robustness against coordinate quantization (in the parentheses are the results of Wang et al. robust watermarking method [26])

Model	Quantization	*corr*	MSDM
	9-bits	0.99 (0.93)	0.12 (0.49)
Venus	8-bits	0.98 (0.70)	0.26 (0.66)
	7-bits	0.97 (0.63)	0.42 (0.79)
	9-bits	0.99 (0.84)	0.09 (0.44)
Rabbit	8-bits	0.99 (0.59)	0.29 (0.61)
	7-bits	0.98 (0.05)	0.53 (0.76)
	9-bits	0.99 (0.61)	0.11 (0.44)
Horse	8-bits	0.97 (0.25)	0.36 (0.60)
	7-bits	0.97 (0.17)	0.51 (0.73)

Table 8 Robustness against the random additive noise $RNA^{amplitude}$, Laplacian smoothing $LS^{numberofiteration}$ and coordinates quantization $CQ^{numberofbitplane}$ (in the parentheses are the results given from Lee et al. [16] watermarking method)

	Horse		Bunny		Venus	
	corr	MRMS	*corr*	MRMS	*corr*	MRMS
$RNA^{0.5\%}$	0.98 (0.91)	0.32 (3.82)	1 (0.93)	0.26 (3.52)	0.99 (0.91)	0.42 (4)
LS^{30}	0.99 (0.96)	0.24 (2.22)	0.99 (0.93)	0.23 (2.35)	0.98 (0.99)	0.37 (2.59)
CQ^{7}	0.97 (0.93)	0.37 (3.18)	0.99 (0.91)	0.31 (3.33)	0.97 (0.77)	0.39 (4.18)

Table 9 Robustness against similarity transformation (Uniform Scaling $US^{(scalingfactor)}$, $T^{(x,y,z)}$ and $R^{Rotationangle(x,y,z)}$)

Models		Bunny	Horse	Rabbit
	MRMS	0.102	0.064	0.152
$US^{(1.5)}$	MSDM	0.66	0.64	0.89
	corr	0.98	0.99	0.992
	MRMS	0.0064	0.005	0.0082
$T^{(0.5,0.5,1.5)}$	MSDM	0.53	0.19	0.23
	corr	1	1	1
	MRMS	0.0105	0.008	0.026
$R^{30°(0.1,0.1,0.1)}$	MSDM	0.58	0.51	0.43
	corr	1	1	1

Table 10 Robustness against connectivity attacks (in the parentheses are the results given from Ai et al. [1] watermarking method)

	Corr	
Model	Bunny	Horse
Mesh simplification		
5%(reduce 21 vertexes)	0.9841 (0.9732)	0.9975
10%(reduce 42 vertexes)	0.9137 (0.8657)	0.9766
20%(reduce 84 vertexes)	0.8641 (0.7595)	0.9274
Cropping		
5%	0.9678 (0.9118)	0.9754
25%	0.8126 (0.7021)	0.8334
simplification(95%)+cropping(10%)	0.7983 (0.6701)	0.8621

Table 11 Execution times for both embedding and extraction stages

	Venus	Rabbit	Horse	Bunny	David	Hand
Embedding time (s)	0.0302	0.0291	0.0297	0.0341	0.0347	0.0339
Extraction time (s)	0.00666	0.00576	0.00612	0.00654	0.00659	0.00661

watermarking method presented in [1] are also shown in the same Table. It is important to note that the authors in [1], employ an existing 2D image watermarking algorithm to embed the watermark information. Their method consists on partitioning a 3D mesh model into Voronoi patches. In the embedding stage, the message is inserted by modifying the vertices in each patch according to its corresponding range image. From the results reported in Table 10, we can notice that the normalized correlation values, obtained by our method, are higher than those obtained by the reference method.

5.5 Complexity evaluation

In order to assess the time complexity of our watermarking scheme, execution-time tests were conducted employing executables generated by Visual Studio 9.0 operating in release mode. The source code was written in C++. All tests were conducted on a laptop with an Intel Core 3 CPU M350 at 2.23 GHz, and operating system Windows 7 SP 1. Table 11 presents the execution times for embedding/extraction stages applied on 6 test models: venus, rabbit, horse, bunny, david head and hand. It is worth mentioning that the added complexity induced by the reordering process has been considered. From the reported results we can deduce that our watermarking system is computationally efficient depending on the number of wavelet coefficient in the third resolution level. The full embedding time varies from 0.0291 and 0.0347 seconds. Based on the same results reported in Table 10 we found that the extraction delay varies between 0.00576 and 0.00659 seconds. Thus the extraction process is five times faster than the watermark insertion.

6 Conclusion

In this paper, we have reported a new blind and high-capacity watermarking framework of 3D meshes. Our watermarking technique consists on extended version of QIM based embedding approach applied to the norms of wavelet coefficient vectors. Experimental results show that despite its simplicity, our approach is characterized by large payload, high visual quality reconstruction, and robustness to several geometric attack scenarios. The invariance to similarity transformation is attained by re-ordering the wavelet coefficient vectors. A satisfying robustness is also achieved against some connectivity attacks.

In our future work, we plan to apply a re-ordering process (vertices and facets) on the original model before irregular wavelet analysis to ensure a good robustness against connectivity re-ordering attacks.

References

1. Ai QS, Liu Q, Zhou ZD, Yang L, Xie SQ (2009) A new digital watermarking scheme for 3D triangular mesh models. Signal Process 89:2159–2170
2. Alface RP, Macq B (2007) From 3D mesh data hiding to 3D shape blind and robust watermarking: A survey. Lect Notes Comput Sci Trans Data Hiding Multimed Syst 2:99–115
3. Aspert N, Santa-Cruz D, Ebrahimi T (2002) Mesh: measuring errors between surfaces using the Hausdorff distance
4. Bogomjakov A, Gotsman C, Isenburg M (2008) Distortion-free steganography for polygonal meshes. Proc Comput Graph Forum 27(2):637–642
5. Cayre F, Macq B (2003) Data hiding on (3-D) triangle meshs. IEEE Trans Signal Process 51(4):939–949
6. Chen B, Wornell GW (2001) Quantization index modulation, a class of provably good methods for digital watermarking and information embedding. IEEE Trans Inf Theory 47(4):1423–1443
7. Chen L, Kong X, Weng B, Yao Z, Pan R (2011) A novel robust mesh watermarking based on BNBW. EURASIP J Adv Signal Process
8. Cheng YM, Wang CM (2006) A high-capacity steganographic approach for 3D polygonal meshes. Int J Comput Graph 22(9):845–855
9. Costa M (1983) Writing on dirty paper. IEEE Trans Inf Theory 29(3):439–441
10. Cox IJ, Miller ML, Bloom JA, Fridrich J, Kalker T (2007) Digital watermarking and steganography. Morgan Kaufmann Publishers Inc. ISBN: 978-0-12-372585-1
11. Chung IL, Chou CM, Tseng DC (2011) A robust high capacity affine-transformation-invariant scheme for watermarking 3D geometric models. Proc J Innov Comput Inf Control 7(6):3419–3435
12. Gao X, Zhang C, Huang Y, Deng Z (2012) Multiresolution analysis for surfaces of arbitrary topological type. ACM Trans Multimed Comput Commun Appl 8
13. Kanai S, Date H, Kishinami T (1998) Digital watermarking for 3D polygon using multiresolution wavelet decomposition. In: Proceedings of sixth IFIP WG 5.2 GEO-6. Tokyo, pp 296–307
14. Kim MS, Valette S, Jung HY, Prost R (2005) Watermarking of 3D irregular meshes based on wavelet multiresolution analysis. Proc Int Work Digit Watermarking (IWDW'05):313–324
15. Lavoué G, Gelasca ED, Dupont F, Baskurt A, Ebrahimi T (2006) Perceptually driven 3D distance metrics with application to watermarking. Proc SPIE Electron Imaging 6312
16. Lee H, Dikici C, Lavoué G, Dupont F (2012) Joint reversible watermarking and progressive compression of 3D meshes. Appl Math Comput 27(6-8):781–792
17. Lin CH, Chao MW, Chen JY, Yu CW, Hsu WY (2013) A high-capacity distortion- free information hiding algorithm for 3D polygon models. Int J Innov Comput Inf Control 9(3):1321–1335
18. Lounsbery M, DeRose TD, Warren J (1997) Multiresolution analysis for surfaces of arbitrary topological type. ACM Trans Graph 16:34–37
19. Maret Y, Ebrahimi T (2004) Data hiding on (3D) polygonal meshs. In: Proceedings of ACM multimedia and security workshop. Magdeburg, Germany pp. 68–74
20. Sweldens W (1998) The lifting scheme: a construction of second generation wavelets. SIAM J Math Anal 29(2):511–546
21. Uccheddu F, Corsini M, Barni M (2004) Wavelet-based blind watermarking of 3D models. In: Proceedings of workshop on multimedia and security. ACM Press, pp 143–154
22. Valette S, Prost R (2004) Multiresolution analysis of irregular surface meshes. IEEE Trans Vis Comput Graph 10:113–122
23. Wang CM, Cheng YM (2005) An efficient information hiding algorithm for polygon models. Comput Graph Forum 24(3):591–600
24. Wang CM, Cheng YM (2006) Watermarking mesh-based representations of 3-D objects using local moments. IEEE Trans Image Process 15(3):687–701
25. Wang Z, Bovik A, Sheikh H, Simoncelli E (2004) Image quality assessment: from error visibility to structural similarity. Proc IEEE Trans Image Process 13(4):1–14
26. Wang K, Lavoué G, Denis F, Baskurt A (2008) Hierarchical watermarking of semiregular meshes based on wavelet transform. IEEE Trans inf Forensic Secur 3:620–634
27. Wang K, Lavoué G, Denis F, Baskurt A (2008) A comprehensive survey on three-dimensional mesh watermarking. Proc IEEE Trans Multimed 10(8):1513–1527
28. Yang S, Yao Z (2010) A data hiding scheme based on local coordinate system for 3D triangle mesh models. J Softw 5(4):437–446

Azza Ouled Zaid received the Electrical received the Eng. degree in electronic from the National Engineering School of Sfax, Tunisia, in 1998 and the M.Sc. degree in Captors and Instrumentation for Vision Systems from L3I Laboratory, the Rouen University, France, in 1999, and the Ph.D. degree in Electronic Sciences in 2002 from the University of Poitiers, Poitiers, France. In 2003-2004 she was a Postdoctoral Fellow with LSS Laboratory from SUPELEC Engineering school in Paris France. Currently, she is Associate Professor at the High Computer Science Institute of Tunis, Tunisia. Since September 2004, she is a member of the Communication Systems Laboratory of National Engineering School of Tunis Tunisia, and she is Research team leader in the same Laboratory from 2009. Her research interests include multimedia signal processing, scalable image and video coding, 3D mesh coding, watermarking and indexing.

Meha Hachani received the a masters degree in computer science from the Sciences Faculty of Tunis, Tunisia, in 2010, and the M.Eng.Sc. degree in engineering from the National Engineering School of Tunis, in 2012. Currently she is pursuing the Ph.D. degree in Telecommunications at the National Engineering School of Tunis, the University of Tunis El Manar, Tunis, Tunisia. Her current research interests include 3D mesh coding and indexing.

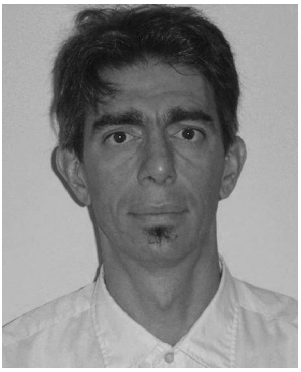

William Puech received the diploma of Electrical Engineering from the University of Montpellier, France, in 1991 and the Ph.D. Degree in Signal-Image-Speech from the Polytechnic National Institute of Grenoble, France in 1997. He started his research activities in image processing and computer vision. He served as a Visiting Research Associate to the University of Thessaloniki, Greece. From 1997 to 2000, he had been an Assistant Professor in the University of Toulon, France, with research interests including methods of active contours applied to medical images sequences. Between 2000 and 2008, he had been Associate Professor and since 2009, he is full Professor in image processing at the University of Montpellier, France. He works in the LIRMM Laboratory (Laboratory of Computer Science, Robotic and Microelectronic of Montpellier). His current interests are in the areas of protection of visual data (image, video and 3D object) for safe transfer by combining watermarking, data hiding, compression and cryptography. He has applications on medical images, cultural heritage and video surveillance. He is the head of the ICAR team (Image & Interaction) and he has published more than 15 journal papers, 8 book chapters and more than 80 conference papers. W. Puech is associate editor of J. of Advances in Signal Processing, Springer and he is reviewer for more than 15 journals (IEEE Trans. on Image Processing, IEEE Trans. on Multimedia, IEEE TCSVT, IEEE TIFS, Signal Processing: Image Communication,...) and for more than 10 conferences (IEEE ICIP, EUSIPCO,...)